

Review

Advanced MXene-Based Micro- and Nanosystems for Targeted Drug Delivery in Cancer Therapy

Fatemeh Mohajer ¹, Ghodsi Mohammadi Ziarani ^{1,*}, Alireza Badiiei ², Siavash Iravani ³
and Rajender S. Varma ^{4,*}

¹ Department of Organic Chemistry, Faculty of Chemistry, Alzahra University, Tehran 19938-93973, Iran

² School of Chemistry, College of Science, University of Tehran, Tehran 14176-14411, Iran

³ Faculty of Pharmacy and Pharmaceutical Sciences, Isfahan University of Medical Sciences, Isfahan 81746-73461, Iran

⁴ Regional Centre of Advanced Technologies and Materials, Czech Advanced Technology and Research Institute, Palacký University in Olomouc, Šlechtitelů 27, 783 71 Olomouc, Czech Republic

* Correspondence: gmohammadi@alzahra.ac.ir (G.M.Z.); varma.rajender@epa.gov (R.S.V.)

Abstract: MXenes with unique mechanical, optical, electronic, and thermal properties along with a specific large surface area for surface functionalization/modification, high electrical conductivity, magnetic properties, biocompatibility, and low toxicity have been explored as attractive candidates for the targeted delivery of drugs in cancer therapy. These two-dimensional materials have garnered much attention in the field of cancer therapy since they have shown suitable photothermal effects, biocompatibility, and luminescence properties. However, outstanding challenging issues regarding their pharmacokinetics, biosafety, targeting properties, optimized functionalization, synthesis/reaction conditions, and clinical translational studies still need to be addressed. Herein, recent advances and upcoming challenges in the design of advanced targeted drug delivery micro- and nanosystems in cancer therapy using MXenes have been discussed to motivate researchers to further investigate this field of science.

Keywords: MXene-based systems; nanocomposites; cancer nanotherapy; photothermal therapy; targeted drug delivery



Citation: Mohajer, F.; Ziarani, G.M.; Badiiei, A.; Iravani, S.; Varma, R.S.

Advanced MXene-Based Micro- and Nanosystems for Targeted Drug Delivery in Cancer Therapy.

Micromachines **2022**, *13*, 1773.

<https://doi.org/10.3390/mi13101773>

mi13101773

Academic Editor: Nityasagar JENA

Received: 13 September 2022

Accepted: 17 October 2022

Published: 19 October 2022

Publisher's Note: MDPI stays neutral with regard to jurisdictional claims in published maps and institutional affiliations.



Copyright: © 2022 by the authors. Licensee MDPI, Basel, Switzerland. This article is an open access article distributed under the terms and conditions of the Creative Commons Attribution (CC BY) license (<https://creativecommons.org/licenses/by/4.0/>).

1. Introduction

Today, the development of nanotechnology has resulted in the creation of several multidisciplinary research domains, namely bionanotechnology, with special contributions in biomedicine and cancer nanomedicine [1–6]. An assortment of nanoparticles and nanoarchitectures has been designed with satisfactory biocompatibility and targeting properties for a wide range of biomedical and clinical applications; however, due to the stringent regulatory necessities, only a handful of them have entered into clinical trials/studies. Nevertheless, these materials have garnered widespread attention from scientists for their deployment as anticancer nanocarriers and nanobiosensors [7–12].

Chiral peptide/protein-derived supramolecules with biological activities can assist in prevention and treatment of various diseases, especially cancers [13]. Biomedicine entails ground-breaking supplies and technologies for specific therapeutics. Traditional policies are not in favor relative to modern medicine due to vital shortcomings, such as nonexact targeting, as well as the absence of synergistic attributes, wherein the booming development of nanotechnologies brings forth a fresh outlook to the biomedicine arena [14–16]. In this context, the design of nanomaterials with therapeutic and diagnostic potential has been widely noticed by researchers. For instance, two-dimensional (2D) hexagonal boron nitride (2D h-BN) flatlands have garnered much attention due to the optical and physicochemical properties, outstanding thermal/chemical constancy, and biocompatibility [17,18], showing excellent potential in biomedicine [19].

On the other hand, with the discovery of graphene [20], transition metal dichalcogenides (e.g., TiS_2 , MoS_2 , and WS_2) [21–23], black phosphorus nanosheets [24], layered double hydroxides [25], graphitic carbon nitride [26], boron nitride [27], metal–organic frameworks [28], and transition metal oxides [29], among others, a variety of advanced micro- and nanosystems have been designed for cancer therapy. Recently, MXenes, 2D material comprising transition metal carbides, nitrides or carbonitrides, have captured widespread attention in photothermal therapy (PTT) in view of the high light-to-heat conversion efficiency, elevated paramagnetic performance, and large specific surface area [30–32]. However, MXene photothermal agents (PTAs) are unstable in aqueous/oxidative surroundings as their terminal functional groups ($-\text{F}$, $-\text{OH}$, or $-\text{O}$) are vulnerable to oxidation and tend to aggregate in physiological solutions; although, after suitable modification/functionalization, the stability and properties of these structures can be improved [33].

Among the recently introduced materials, MXenes are two-dimensional (2D) transition metal carbides and nitrides with a vast surface area and hydrophilicity, which have been explored in biomedical engineering and medicine [34–36]. They have swiftly become popular for a range of study domains due to their outstanding features since Yury Gogotsi and colleagues synthesized the first family member in 2011 [37]. Although MXenes are a relatively young family of 2D materials, the number of scientific articles connected to them nearly doubles every year [30,38–41].

Two-dimensional MXenes are contemporary 2D transition metal carbides, which resemble graphene sheets comprising the formula $\text{M}_{n+1}\text{X}_n\text{T}_x$ (e.g., $\text{Ti}_3\text{C}_2\text{T}_x$). Exfoliation of the “A” layer from a “MAX” predecessor—where M, A, and X indicate the transition metal, elements from IIIA or IVA, and N, respectively—can be used to make these materials, depending on their situation and type of applications. Among widely developed methods deployed for the manufacturing of MXenes comprise urea glass (e.g., Mo_2C and Mo_2N) [42], chemical vapor deposition (e.g., Mo_2C) [43], molten salt etching (e.g., $\text{Ti}_4\text{N}_3\text{T}_x$) [44], hydrothermal fabrication (e.g., $\text{Ti}_3\text{C}_2\text{T}_x$) [45], and electrochemical synthesis (e.g., Ti_2CT_x). The wet etching method, in particular, may be utilized to create them in good quality with largely hydrophilic properties [46]. MXenes and their derivatives can be applied for photothermal and photodynamic cancer therapy [47]. These materials with unique optical properties have been explored in the field of (bio)imaging and (bio)sensing [48–50]. On the other hand, routinely applied anticancer drugs for chemotherapy may suffer from low specificity/selectivity, high toxicity, off-target toxic effects, and inappropriate clearance. Designing multifunctional systems with high biocompatibility, specificity/selectivity, biodistribution, and bioavailability can help to improve the efficiency of cancer therapy and tumor ablation. MXene-based micro- and nanosystems have been applied for targeted delivery of anticancer drugs/therapeutic agents in cancer therapy after surface functionalization/modification by bioactive/biocompatible agents (Figure 1) [51,52].

In addition, long-acting therapeutic anticancer drugs may cause possible toxic effects on normal cells along with a low efficacy in cancer therapy [53–55]. Low bioavailability of conventional chemotherapy, with some drawbacks, such as possible side effects, high dose requirements, and multidrug resistance, have prompted researchers to find new solutions based on drug delivery micro- and nanosystems with the benefits of higher solubility, specific targeting, high biocompatibility, selectivity, and reduced toxicity [56,57]. Conventional organics with biodegradable attributes and strong biocompatibility have been extensively studied for clinical applications, but their poor thermal and chemical stability and low functionality are some of the obstacles limiting their clinical developments [58]. In this context, MXene-based nanostructures have unveiled a variety of clinical and biomedical potential owing to their unique physicochemical properties, such as ease of functionalization, tunable structures, biosafety, and physiological constancy [59]. However, crucial aspects of toxicity and biocompatibility ought to be further explored. The potential toxicity of MXenes has been investigated throughout the embryonic and angiogenesis phases, wherein they have revealed negative impacts during the early stages of embryogenesis [58]; about 46% of MXene-exposed embryos died within 15 days [60]. MXenes were shown to impede the

angiogenesis of the embryo's chorioallantoic membrane after 5 days at the tested dosages. When compared to the controls, several genes were deregulated in the liver tissues and brain of embryos treated with MXene; nevertheless, further research and analysis are warranted to comprehend the potential toxicity of MXenes [60,61]. The biosafety of MXenes can be improved by applying suitable functionalization and hybridization techniques using biocompatible and biodegradable agents (e.g., cellulose and chitosan) along with optimized reaction/synthesis conditions.

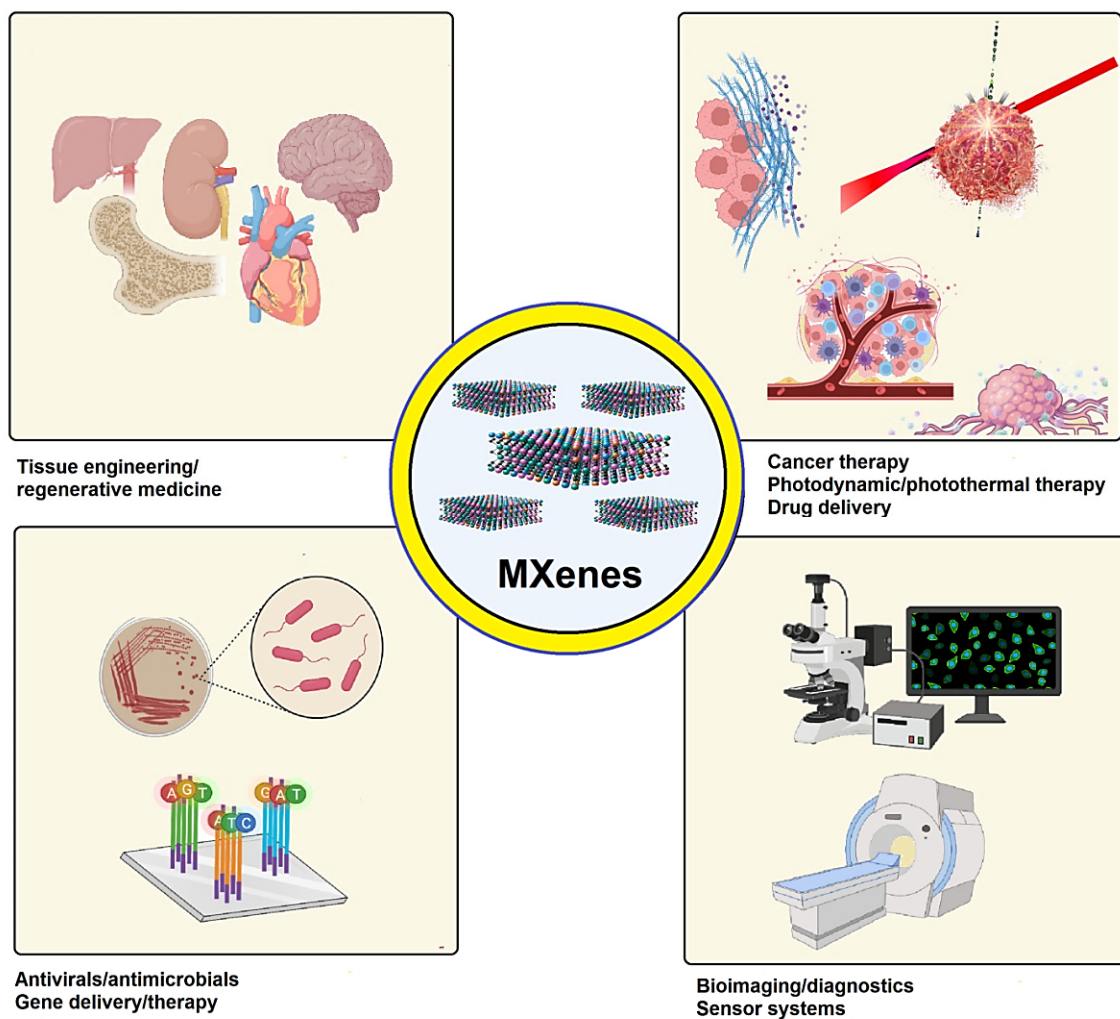


Figure 1. MXenes and their derivatives with versatile biomedical potentials.

The key applications of MXenes in biomedicine comprise, among others, (bio)imaging, tissue engineering, (bio)sensing, cancer therapy/diagnosis, and drug delivery [62,63]. Properties of MXenes can be improved by using suitable hybridization techniques, providing MXenes with improved thickness and compactness of the silane film, uniformity, good density, and fewer flaws [64,65]; wherever conductivity is essential for interaction with electromagnetic waves, interference shielding may exploit appropriate magnetic dipoles. Additionally, 2D MXenes ranging from metallic to semiconductor can detect adjustable conductivity; 2D MXenes with hydrophilicity ought to be manufactured using cost-effective methods [64]. Their layered structures, on the other hand, are likely to hinder the creation of gaps, which may change their magnetic and electric characteristics. As a result, unfavorable effects on the electromagnetic interference activity of composites made from MXenes are not unlikely. This significant disadvantage could be resolved by synergistic interactions amongst MXenes and conducting/magnetic materials [64,66].

Studies on these materials expose the need of controlling their physicochemical characteristics through surface charge engineering for novel biotechnological and biomedical applications [67]. For cancer therapy and tissue-engineering purposes, MXene-based micro- and nanosystems offer adjustable mechanical properties, excellent photothermal conversion efficiency, targeting competence, biocompatibility, selectivity, and regulated drug discharge [68]. For instance, composite hydrogels based on Ti_3C_2 MXene and cellulose have been engineered to respond quickly to near-infrared (NIR)-stimulated features. These manufactured hydrogels modified with doxorubicin (DOX) hydrochloride exhibited exceptional drug release acceleration and could be employed as nanoplatforams for intratumoral cancer therapy [68].

2. Advanced MXene-Based Micro- and Nanosystems

2.1. Structural, Chemical, and Electronic Properties of MXenes

MXenes have functional groups such as F, OH, and O after its exfoliation from the MAX phase where the O- and/or OH- terminated groups are the most stable, as F group will be substituted with OH groups on rinsing and storing in H_2O [69]. Xie et al. stated that OH groups could be transformed into O terminations over high-temperature and/or metal adsorption procedures [69]. In addition, O-terminated MXene could decompose into bare MXene up on interaction with Mg, Ca, Al, or other metals [70]. Modeling is crucial in designing MXenes with novel structures [71]. Surface groups are located above the hollow sites among three near C atoms [72,73]. The precise configurations of surface groups depend on both, their species and the MXene's constituent materials [74]. MXenes have many usage such as, electronic [75], dielectric [76], magnetic [77–80], elastic [81], thermoelectric [82], and optical properties [83] as has been documented by computational studies. Bare MXene, such as $\text{Ti}_{n+1}\text{X}_n$, are known to be metallic in behavior [83]. In terms of X atoms, titanium nitrides exhibit more metallic properties than titanium carbides, simply because the N atom possesses one more electron than the C atom [84]. In terms of the chemical properties of MXenes, Naguib et al. reported that $\text{Ti}_3\text{C}_2\text{T}_x$ are oxidized in air, CO_2 , or pressurized water [85] wherein the oxidation results in the formation of anatase TiO_2 nanocrystals embedded in amorphous carbon sheets (TiO_2 -C hybrid structure).

One of interesting topics in the progression of theranostic nanomedicines for in vivo clinical studies is the finding of association among the physicochemical nature of the designed structures and their connections with living organizations. Therefore, experimental studies are necessary to assess the productivity, toxic effects, and their physio-chemical properties. Comprehensive preclinical studies and the assessment of the biological interactions of MXenes and their complexes in in vivo systems could support to find their limits in the future [86].

MXenes are important due to their widespread applications as supercapacitors [87], in electromagnetic interference shielding [88], optical and light detection [89], and even in communication and biology [90]. The optical properties of MXenes have displayed the possibility of producing electrodes [90], photonic devices and plasmonic applications [91]. Furthermore, biocompatible MXene (Ti_3C_2)-based composites ($\text{MnO}_x/\text{Ti}_3\text{C}_2$) were applied for cancer theranostics, nanoplatforam for photothermal cancer/tumor nanotherapy by photoacoustic imaging [92].

2.2. MXene-Based Biomimetic Plasmonic Method

An effective plasmonic-enhanced technique has been presented and used for biomimetic photo-induced plasmonic assembly (NPD@M). Nb_2C plasmon (MXene), Pt nanozymes, DOX, and tumor cytomembrane make up the assemblage for targeted cancer therapy. The hot-electrons created from MXene after homogeneous targeting and internalization into cancer cells notably promote the catalase-like and oxidase-like functions of Pt nanozymes to generate O_2 and reactive oxygen species (ROS), combined with tumor-penetrating photothermal therapy. DOX is also released in acidic conditions, aided by O_2 and ROS-induced suppression of P-glycoprotein (P-gp)-mediated drug efflux [93]. These results demon-

strated that MXene-augmented nanozyme therapy decreased the HeLa cell viability by 38.67% when compared to control cells; nanozyme catalytic activity was improved by the hot-electron oscillations from Nb₂C by NIR-II laser to kill tumors. NPDM was inserted into the body by the tail vein so that it could enter the tumor through the EPR effect and tumor cytomembrane targeting while the NIR-II light illumination and photothermal possessions expanded tumor vessels to improve the blood pressure to a drug eruption. The nanozyme activity was boosted by the plasmon thermoplastic result. Using a high concentration of H₂O₂ high (100 μM~1 mM) in the tumor results in down-regulation of the hypoxia-inducible factor (HIF-1α). Concurrently, the heightened oxidase endorses ROS production which reduces the mitochondrial energy source to P-gp glycoprotein, while a membrane efflux pump recognizes the chemotherapeutic drugs for transporting out of cells. This process counters multidrug resistance and recovers the chemotherapy effectiveness. Collectively, biomimetic plasmonic assembly completes the tumor treatment by irradiation of NIR-II, as a novel strategy to promote the nanozyme biocatalyst and plasmonic application in tumors (Figure 2) [94].

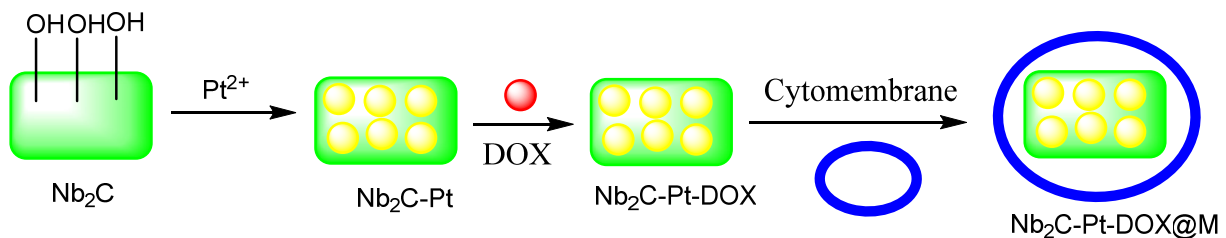


Figure 2. Schematic diagram of MXene-based biomimetic plasmonic assembly for targeted cancer therapy [94].

2.3. MXene/DOXjade Platforms

For synergistic cancer therapy, Ti₃C₂-PVP@DOXjade, a pH-responsive dual-therapeutic compound based on deferasirox and DOX, was created wherein photo-irradiation with Ti₃C₂-PVP@DOXjade displayed a pH-responsive iron chelation/PTT/chemotherapy anticancer activity [95]. Cancer cells have a high requirement for iron with important roles in cell proliferation, tumor growth, and metastasis thus rendering iron metabolism a promising therapeutic target. Unfortunately, existing iron-based therapy techniques are frequently ineffective and have side effects. The prodrug combines deferasirox (ExJade[®]), a therapeutically authorized iron chelator, with DOX, a topoisomerase 2 inhibitor (DOX). DOXjade was loaded onto ultrathin 2D Ti₃C₂ MXene nanosheets to create Ti₃C₂-PVP@DOXjade, which allows DOXjade's iron chelation and chemotherapeutic functions to be photo-activated at tumor sites, additionally potentiating a robust photothermal effect with photothermal conversion efficiencies up to 40%. Ti₃C₂-PVP@DOXjade promotes apoptotic cell death and down-regulates the iron depletion-induced iron transferrin receptor, according to antitumor mechanistic studies as iron chelation/photothermal/chemotherapy responds to the pH of the tumor [95].

Two-dimensional ultrathin Ti₃C₂ MXene nanosheets were predicted to react with DOXjade in this setting. The ensuing construct, known as Ti₃C₂-PVP@DOXjade, was projected to have high photothermal efficiency [96]. Indeed, when exposed to NIR light at 808 nm inside the optical-therapeutic window (650–900 nm), Ti₃C₂ nanosheets included in Ti₃C₂-PVP@DOXjade demonstrated photothermal conversion efficiencies up to 40% and bestowed a good PTT performance [97,98]. Furthermore, Ti₃C₂-PVP@DOXjade flaunted a sensitive tumor pH-responsive iron chelation/PTT/chemotherapy anticancer impact. To remove the Al layer, Ti₃AlC₂ Max phase crystals were etched in an aqueous HF solution to generate Ti₃C₂ which was treated with an aqueous tetrapropylammonium hydroxide (TPAOH) solution and after agitation, the multilayer Ti₃C₂ nanosheets were formed. MXenes nanosheets and PVP (polyvinylpyrrolidone) were mixed in phosphate-buffered saline to afford Ti₃C₂-PVP; notably, the DOXjade was produced via the modification of DOX

to offer hydrazones [99]. In phosphate-buffered saline (PBS) at pH = 7.4, DOXjade was loaded on Ti_3C_2 -PVP under an argon atmosphere to afford DOXjade-loaded Ti_3C_2 -PVP (Figures 3 and 4).

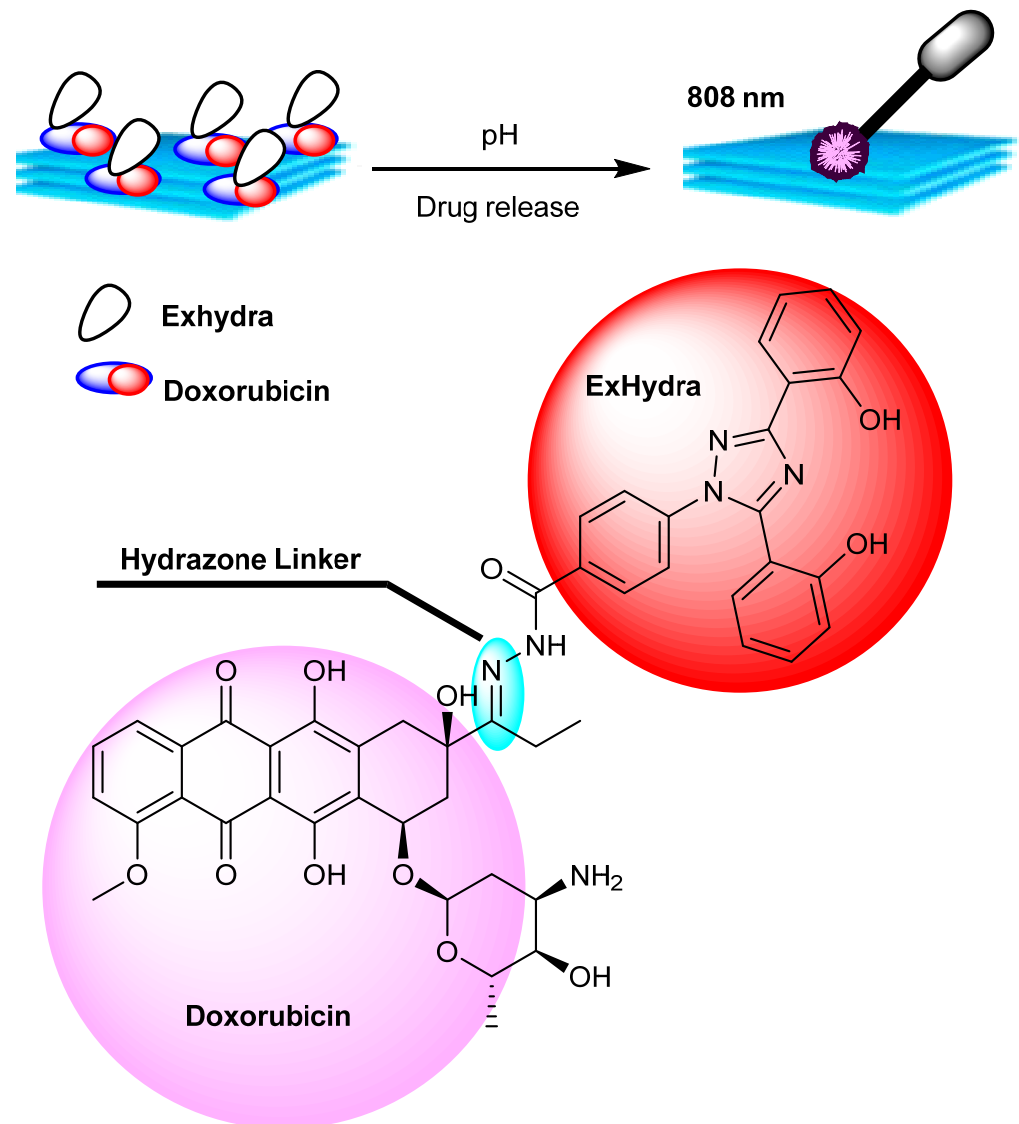


Figure 3. Synthesis of 2D-ultrathin MXene/DOXjade platforms for targeted cancer therapy [95].

2.4. Ti_3C_2 Nanosheet-Based Camouflaged Bionic Cascaded-Enzyme Nanoreactor

The use of enzymes to generate ROS at tumor locations has emerged as a new technique for controlling intracellular redox states in anticancer therapy. The Ti_3C_2 nanosheet-based camouflaged bionic cascaded-enzyme nanoreactor has been applied for combined tumor enzyme dynamic treatment (EDT), phototherapy, and deoxygenation-activated chemotherapy [100]. The deoxygenation-activated drug tirapazamine (TPZ) was loaded onto Ti_3C_2 nanosheets, glucose oxidase (GOX), and chloroperoxidase (CPO) to furnish Ti_3C_2 -GOX-CPO/TPZ (TGCT) which was implanted into nanosized cancer cell-derived membrane vesicles with high-expressed CD47 (meTGCT). The cascade reaction of GOX and CPO, into tumor cells, might create HClO for the effective EDT. Simultaneously, additional laser irradiation would speed up the enzymic-catalytic reaction rate and boost singlet oxygen production (1O_2). A local hypoxic environment combined with EDT-induced oxygen depletion activates a deoxygenation-sensitive prodrug for treatment. Therefore, the synergistic therapeutic benefits of tumor phototherapy, EDT, and chemotherapy are

increased in meTGCT. This cascaded-enzyme nanoreactor affords a good method to bring in anticancer treatment (Figure 5A) [100]. TGCT nanocascaded enzymes were created through the reaction of GOX and CPO onto Ti_3C_2 nanosheets with TPZ drug loading and the biomimetic alteration of CD47-overexpressed cancer cell membrane offer a bionic cascaded-enzyme nanoreactor (as meTGCT). MeTGCT was affected by tumor cells and the enzyme consumes glucose and oxygen in tumor areas to generate the lethal HClO. Under NIR laser irradiation, Ti_3C_2 may create both, heat, and ROS, where heat can speed up the enzyme-catalyzed reaction rate and ROS generation, exacerbating the hypoxic state in the target tumor environment (TME). Then, as a hypoxia-activated prodrug, TPZ is activated by reductase, causing DNA breakage and cell death, thus enhancing EDT and phototherapy effects. As a result, hypoxia-activated chemotherapy may achieve magnified synergistic effects in this camouflaged cascaded-enzyme nanoreactor, effectively inhibiting tumor development [100] (Figure 5B).

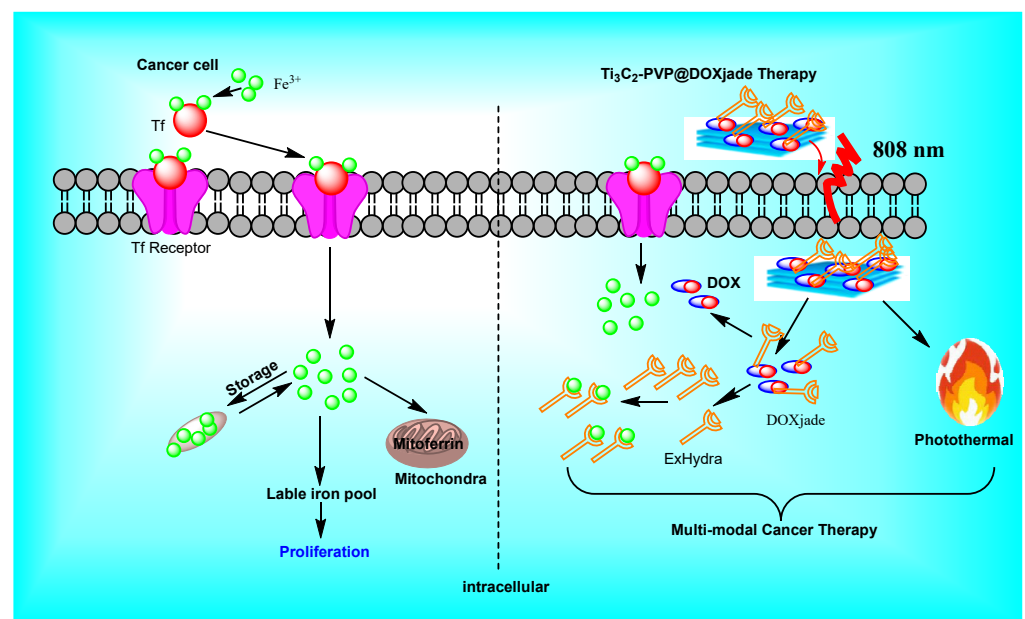


Figure 4. A plausible mechanism of 2D-ultrathin MXene/DOXjade platform for cancer therapy [95].

2.5. Few-Layered Nb_2C (FNC) for Osteoclastogenesis Suppression Inhibited Inflammation and Osteoclastogenesis

Implant-derived particulates, such as ultra-high molecular-weight polyethylene (UHMWPE), activate the immune system to phagocytose particles, resulting in the production of ROS [101]. ROS stimulates osteoclast genesis and causes macrophages to release cytokines, which aid in the progression of osteolysis. The few-layered Nb_2C (FNC) is an antioxidant with the ability to reduce cytokine production and inhibit osteoclast genesis by ROS adsorption. Furthermore, in a mouse calvarial model, local injection of a few-layered Nb_2C (FNC) reduces UHMWPE and induced osteolysis. As a result, it has been demonstrated that FNC could be beneficial in the treatment of osteolytic bone disease encouraged by excessive osteoclast genesis. In this process, the reaction of Nb_2AlCl_5 , LiF, and HCl provided bulk Nb_2C (BNC) which was treated with tetrapropylammonium hydroxide (TPAOH) to offer FNC. The ensuing product (few-layered Nb_2C) was washed with DI water, centrifuged, and dried. It was demonstrated that FNC was effective in scavenging ROS for treating ROS-related diseases via FNC adsorption of ROS in the process of osteoclast genesis suppression *in vitro*. Furthermore, the findings displayed that osteolysis was condensed *in vivo* when UHMWPE was stimulated (Figure 6) [101].

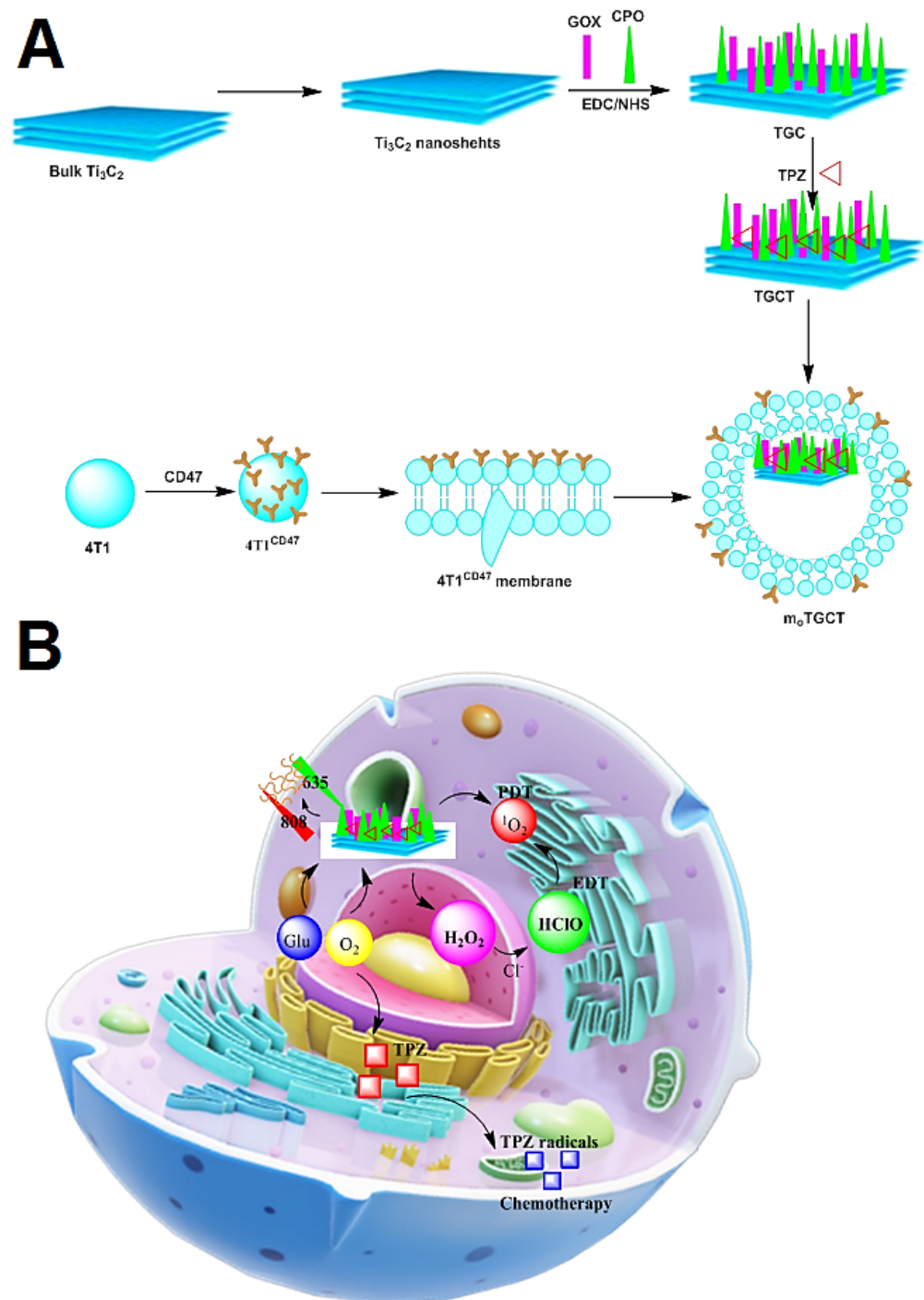


Figure 5. (A) Schematic diagram of Ti_3C_2 nanosheet-based camouflaged bionic cascaded-enzyme nanoreactor. (B) The possible mechanism of action for the designed MXene-based camouflaged bionic cascaded-enzyme nanoreactor (in vivo) [100].

2.6. Advanced Systems Based on Ti_3C_2 MXenes

Titanium carbide (Ti_3C_2) MXenes were developed by surface modification in the presence of antioxidants (sodium ascorbate, SA, and dopamine, DA) to obtain (DA/SA@ Ti_3C_2 = DSTC) [33]. Antioxidants improved the MXenes stability by trapping oxidants and the MXenes functionalization process with biotic molecules, therefore glucose oxidase (GOx) and photosensitizer (chlorin e6 = Ce6 PS) were attached to the DSTC surface through the carbodiimide link to provide Ce6/GOx@SDTC = CGDSTC). It was applied for glucose deprivation and photodynamic therapy for the co-killing of cancer cells. Increasing

the solution temperature by laser irradiation boosted the enzymatic activity of CGDSTC nanosheets. These nanosheets exhibited cytocompatibility to HePG2 and HeLa cells; it was established that 90% of cells were killed by glucose and laser irradiation through the cooperative outcome between famine therapy and phototherapy. The possible mechanisms of synthesized CGDSTC nanosheets are illustrated in Figure 7A [33]. Glucose-rich environments provide gluconic acid in the tumor by GOx, subsequently sensitizing the tumor cells to photothermal properties by limiting the tumor glycolytic path. Photo irradiation with 808 and 671 nm lasers participates in tumor cell destruction by supporting Ti_3C_2 - mediated PTT and Ce6-mediated PDT properties; higher temperature produces tumor oxygen levels alongside with GOx. Accordingly, synthesized CGDSTC nanosheets by starvation and phototherapy, remove the tumor cells more safely. The enzyme (GOx) and photosensitizer (Ce6) were sequentially conjugated onto the DSTC nanosheets via carbodiimide coupling between the carboxyl groups and amine groups of DSTC nanosheets to attain CGDSTC nanosheets with photodynamic and starvation properties (Figure 7B) [33].

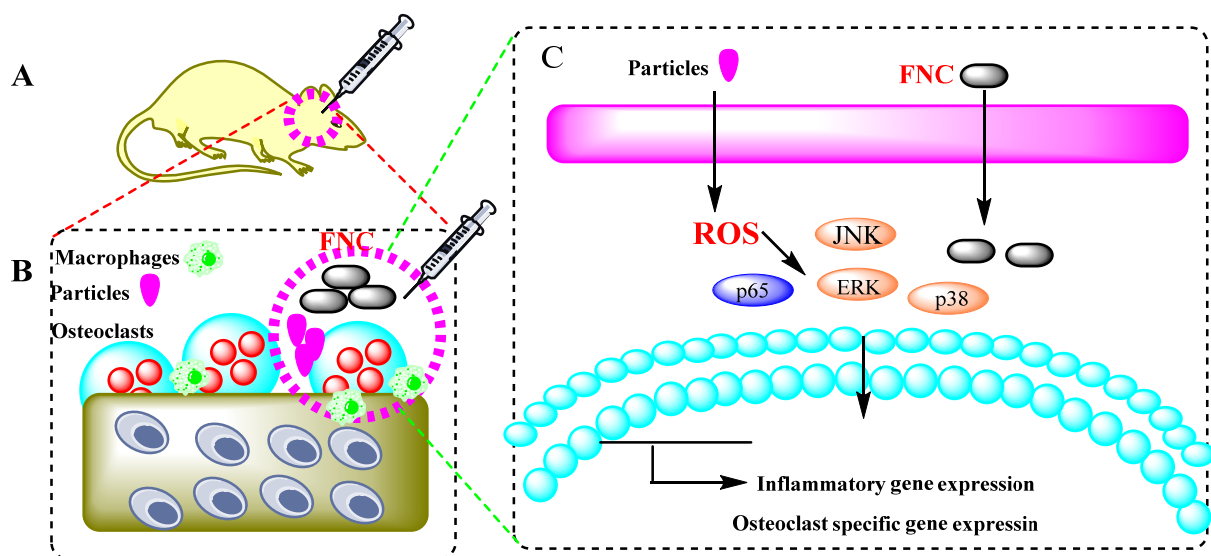


Figure 6. A schematic diagram of FNC inhibited inflammation and osteoclastogenesis. (A) Local injection of FNC at osteolytic sites. (B) Materials interaction between macrophages and osteoclasts influenced inflammation and osteoclastogenesis. (C) FNC was phagocytosed, and FNC exhibited the effect of ROS adsorption. Subsequently, the inflammatory and osteoclast-specific genes were down-regulated [101].

Through the fluorescence imaging, MXene-based multifunctional nanosheets were developed to expand high cancer therapeutic efficacy via the cooperative effect. The stability of Ti_3C_2 MXene was improved by surface modification with the antioxidants such as sodium ascorbate (SA) and dopamine (DA) to offer DA/SA@ Ti_3C_2 (abbreviated as DSTC).

2.7. MXene Quantum Dot/ZIF-Based Systems for Anticancer Drug Delivery

Designing novel stimuli-responsive multifunctional structures for targeted drug delivery in cancer therapy has been studied [102,103]. For instance, zeolitic imidazolate framework-8 (ZIF-8) with a large and precise surface expanse, encapsulates DOX and MXene quantum dot (MQD) to furnish MQD@ZIF-8/DOX with high photothermal conversion efficacy and ROS generation ability to provide excellent photothermal therapy and photodynamic therapy effects. In addition, DOX was loaded into MQD@ZIF-8 nanoparticles which released the DOX at pH 5.6. Multifunctional MQD@ZIF-8 drug delivery is illustrated in Figure 8, where Zn^{2+} was immobilized on MQD as nucleation nodes. MQD@ZIF-8 composites were synthesized in situ via the rapid reaction between Zn^{2+} and 2-MIM molecules. The anticancer drug, DOX, was encapsulated in MQD@ZIF-8 where MQD served as PTA

and PS in this system to realize combined PDT/PTT therapy, which rapidly converted NIR light energy to ablative heat and generated ROS under UV laser irradiation to kill cancer cells. Moreover, DOX release could be markedly increased under the tumor environment. The MQD@ZIF-8/DOX nanocarrier can therefore achieve the effect of combined chemotherapy and phototherapy during tumor treatment [102,103].

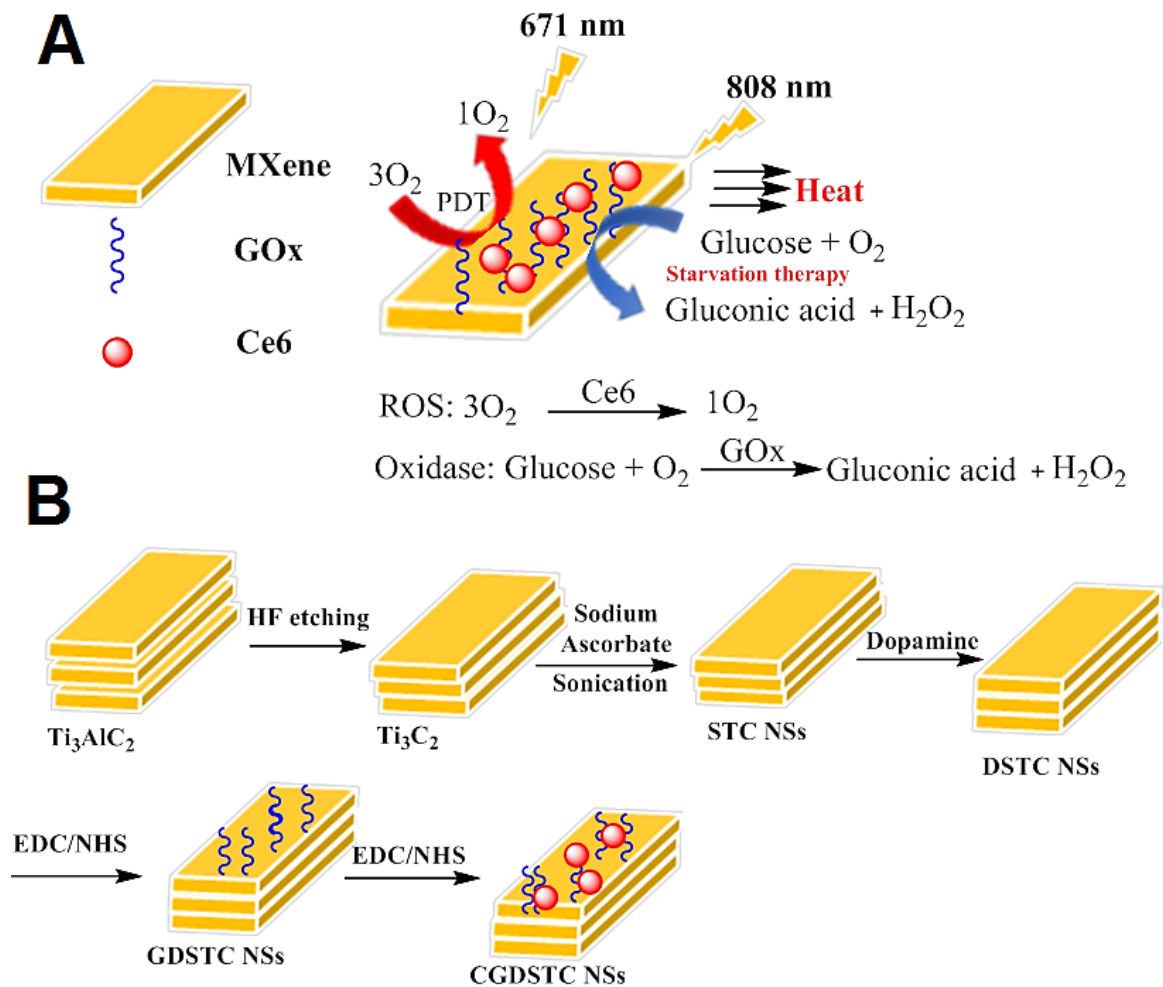


Figure 7. (A) Pictorial representation for the working mechanism of CGDSTC nanosheets. (B) The preparative process of CGDSTC nanosheets [33].

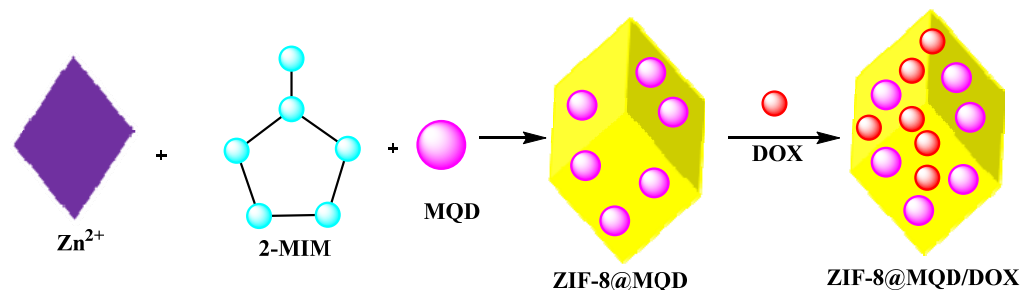


Figure 8. The preparative process of MXene quantum dot/ZIF-based systems for anticancer drug delivery [97].

Multifunctional MQD@ZIF-8 drug delivery system was prepared by instantaneously capturing MQD with phototherapeutic potential and the chemotherapeutic drug DOX in a ZIF-8 environment. The MQD@ZIF-8 nanocarrier had a modest preparation and proficiently linked pH with NIR dual responsiveness to excite the drug release. Through the cell test, it

was illustrated that MQD@ZIF-8 had a greater biocompatibility, and MQD@ZIF-8 could produce temperature and ROS around cells under 808 nm laser and UV irradiation for killing HeLa cells, individually. Thus, MQD@ZIF-8 could be considered as a suitable platform with superb tumor therapeutic potential.

2.8. Ionic Liquid-Exfoliated $Ti_3C_2T_x$ MXene ((IL)- $Ti_3C_2T_x$ MXene) Nanosheets in Cancer Treatment

$Ti_3C_2T_x$ MXenes with potential activity in cancer treatment were produced through an ionic liquid (IL) stripping process; DOX was loaded into (IL)- $Ti_3C_2T_x$ MXene to provide composites with pH-responsive behavior and photosensitivity with enhanced drug release upon 808 nm laser irradiation [104]. These nanocomposites exhibited high chemical stability and good biocompatibility. They could inhibit tumor growth using synergistic photothermal therapy and chemotherapy; photoacoustic imaging has great potential in cancer treatment (Figure 9) [104].

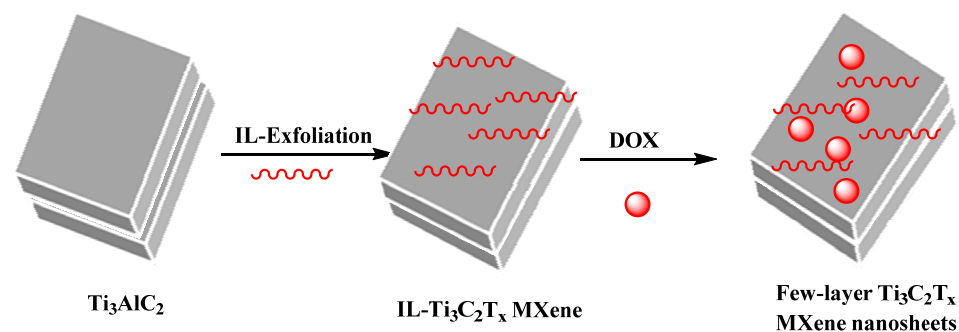


Figure 9. The preparation of few-layer $Ti_3C_2T_x$ MXene nanosheets with high chemical stability using an IL-assisted exfoliating (red patterns) method for photoacoustic imaging-guided synergistic photothermal/chemotherapy of tumors [104].

IL-supported exfoliation of the MXene phase could provide few-layer IL- $Ti_3C_2T_x$. Under 808 nm laser irradiation, the IL- $Ti_3C_2T_x$ MXene nanosheets exhibited high chemical stability and robust near-infrared absorption, with suitable photothermal conversion efficiency. The IL- $Ti_3C_2T_x$ MXene nanosheets could be applied for targeted delivery of DOX with pH-/photosensitivity; the drug release was enhanced in an acidic situation under the laser irradiation (808 nm). These nanosheets displayed good photothermal effects on 4T1 cells under 808 nm (in vitro) to obtain the decent photoacoustic image. Furthermore, they exhibited appropriate antitumor properties (in vitro and in vivo). Thus, these MXene-based systems can be considered for photoacoustic imaging and synergistic photothermal/chemotherapy of cancer with high efficiency [104].

2.9. MXene@Au-Polyethylene Glycol Composites Drug Release

MXene@Au-polyethylene glycol composites have been developed as targeted drug delivery systems with a high capacity for loading chemotherapeutic agents (DOX) [105]; these nanosystems exhibited both NIR laser-triggered and pH-responsive drug release modes [106]. Owing to surface modification with thiol polyethylene glycol aldehyde chains (SH-PEG-CHO) connected to the MXene by Au nanoparticles, the system showed improved photothermal stability, biosafety, and histocompatibility during in vivo and in vitro tests. In addition, based on the good photothermal conversion capability of both Au nanomaterials and MXenes, these nanosystems exhibited synergistic photothermal ablation and chemotherapy for tumor/cancer therapy. Their passively targeted release properties also enhanced the cellular uptake of DOX at tumor sites, thus improving the efficiency of the drug. Future explorations ought to move towards designing surface-modified MXene-based drug delivery platforms with high drug-loading capacity, multiple drug release modes, and synergistic therapy, offering new opportunities for targeted cancer therapy and tumor ablation (Figure 10) [106].

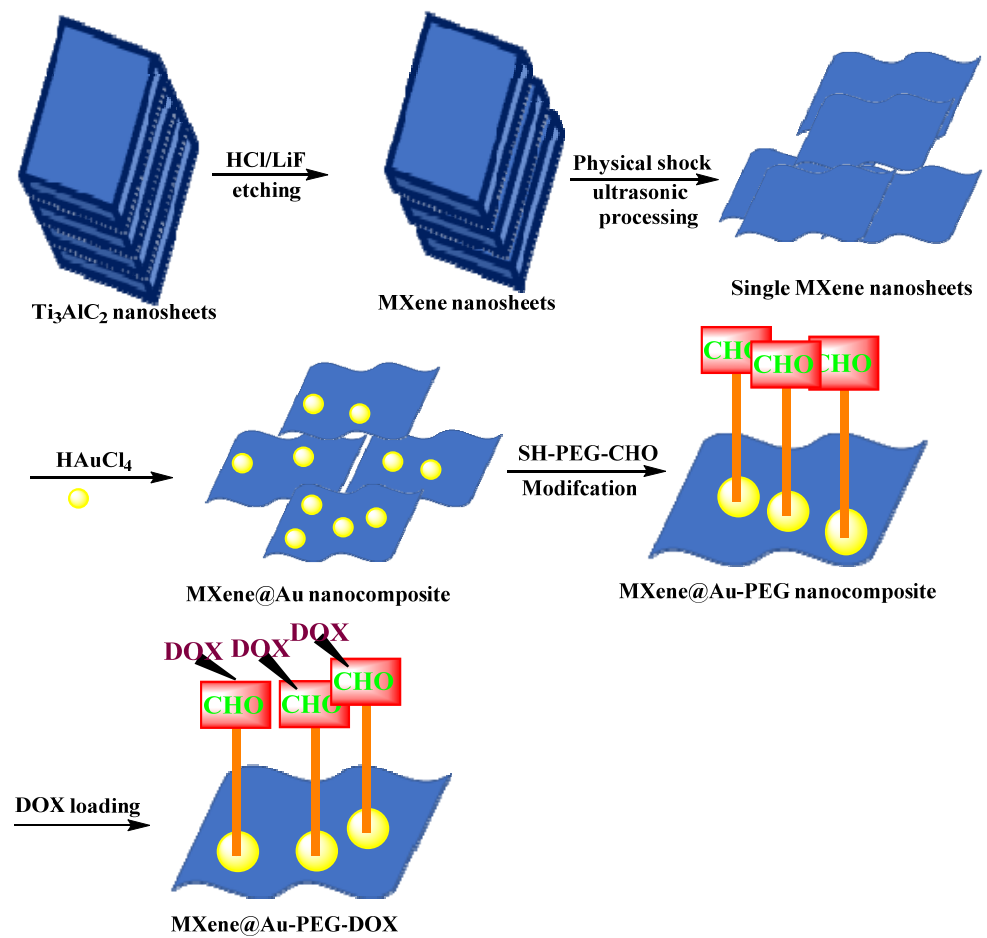


Figure 10. The preparative process and function of designed MXenes for cancer nanotherapy [106].

A variety of MXene-based micro-and nano systems have been designed for targeted cancer therapy (Table 1).

Table 1. Different MXene-based systems for cancer therapy.

Formulations	Targeted Tissue/Organ	Advantages/Benefits	Biocompatibility and Toxicity	Ref.
Nb ₂ C-Pt-DOX@M	Skin	Biomimetic plasmonic assembly completed the tumor treatment by irradiation of NIR-II, as a novel strategy to promote the nanozyme biocatalyst and plasmonic application in tumors.	Bioplasmonic assembly of biocatalyst	[94]
DOXjade-loaded Ti ₃ C ₂ -PVP	Skin	A pH-responsive dual-therapeutic compound based on federation and DOX, was created wherein photo-irradiation with Ti ₃ C ₂ -PVP@DOXjade displayed a pH-responsive iron chelation/PTT/chemotherapy anticancer activity.	Good biocompatibility and lower cytotoxicity	[95]

Table 1. Cont.

Formulations	Targeted Tissue/Organ	Advantages/Benefits	Biocompatibility and Toxicity	Ref.
MeTGCT	Skin	Under NIR laser irradiation, Ti_3C_2 may create both heat and ROS, where heat can speed up the enzyme-catalyzed reaction rate and ROS generation, exacerbating the hypoxic state in the target TME.	Good biocompatibility	[100]
Few-layered Nb_2C (FNC)	bone	Few-layered Nb_2C (FNC) reduces UHMWPE and induced osteolysis.	Good biocompatibility	[101]
CGDSTC nanosheets	Skin	It was applied for glucose deprivation and photodynamic therapy for the cokilling of cancer cells	Higher stability and biologically safe under nonstimulus conditions	[33]
MXene quantum dot/ZIF-based systems	Skin	DOX and MXene quantum dot (MQD) to furnish MQD@ZIF-8/DOX with high photothermal conversion efficacy and ROS generation ability	Good biocompatibility, used as a drug delivery platform.	[97]
Few-layer Ti_3C_2Tx MXene nanosheets	Skin	photoacoustic imaging and synergistic photothermal/chemotherapy of cancer.	Good solubility, nontoxicity	[104]
MXene@Au-polyethylene glycol composites	Skin	Improved photothermal stability, biosafety, and histocompatibility during in vivo and vitro tests.	Good biocompatibility	[106]

3. Conclusions and Perspectives

MXenes, with their intrinsic physicochemical features and superb biocompatibility, have acquired a lot of interest in wide-ranging biological and biomedical applications. By managing preparative constraints, external features could be modified for cancer therapeutics and diagnostics. MXene-based micro- and nanosystems can be applied for targeted delivery of anticancer drugs/therapeutic agents, with the advantages of low toxicity and good biocompatibility. However, the improvement of biocompatibility, pharmacokinetics, and biodegradability of these structures ought to be focused comprehensively; discovering simple, cost-effective, and environmentally benign synthesis/functionalization approaches, optimized synthesis/reaction conditions, and efficient hybridization uniting biocompatible/biodegradable agents, are the key parameters in improving the properties and effectiveness of MXene-based systems. The verification of successful absorption of therapeutic chemicals from the circulation into the desired location is a key challenge in systemic disposition. The vascular endothelial cell, which acts as an obstacle between organs and blood, is one of the most important concerns. Endothelial cells' cellular acceptance of manmade nanosystems is thus critical for their biological and therapeutic applications. MXene-based composites can be functionalized or modified utilizing appropriate functional groups/agents to enhance their loading capacity, biocompatibility, and bioavailability. This strategy can also be adopted to reduce undesirable/adverse side effects as well as probable immune system reactions. MXene-based materials for targeted drug delivery in cancer

therapy would continue their fast progress made in less than half a decade in the future at a rapid pace. Hopefully, the analyses and outlook directions offered in this review can guide scientists and engineers to focus on the development of MXenes and their derivatives for targeted drug delivery and cancer therapy.

Author Contributions: F.M.: writing—review and editing, draw graphical abstract; G.M.Z.: project administration, supervision, writing—review and editing; A.B.: writing—review and editing, supervision; S.I.: writing—review and editing; R.S.V.: writing—review and editing, supervision. All authors have read and agreed to the published version of the manuscript.

Funding: This research received no external funding.

Data Availability Statement: Not applicable.

Acknowledgments: We acknowledge the Research Council of Alzahra University.

Conflicts of Interest: The authors declare no conflict of interest.

References

1. Barry, N.P.E.; Sadler, P.J. Challenges for Metals in Medicine: How Nanotechnology May Help To Shape the Future. *ACS Nano* **2013**, *7*, 5654–5659. [[CrossRef](#)]
2. Iravani, S.; Soufi, G.J. Gold Nanostructures in Medicine and Biology. In *Nanoparticles in Medicine*; Springer: Berlin/Heidelberg, Germany, 2020; pp. 175–183.
3. Iravani, S.; Varma, R.S. Greener synthesis of lignin nanoparticles and their applications. *Green Chem.* **2020**, *22*, 612–636. [[CrossRef](#)]
4. Iravani, S.; Varma, R.S. Green synthesis, biomedical and biotechnological applications of carbon and graphene quantum dots. *A Review. Environ. Chem. Lett.* **2020**, *18*, 703–727. [[CrossRef](#)] [[PubMed](#)]
5. Mohammadi Ziarani, G.; Mofatehnia, P.; Mohajer, F.; Badieli, A. Rational design of yolk–shell nanostructures for drug delivery. *RSC Adv.* **2020**, *10*, 30094–30109. [[CrossRef](#)] [[PubMed](#)]
6. Mohajer, F.; Mohammadi Ziarani, G.; Badieli, A. New advances on Au–magnetic organic hybrid core–shells in MRI, CT imaging, and drug delivery. *RSC Adv.* **2021**, *11*, 6517–6525. [[CrossRef](#)]
7. Soufi, G.J.; Iravani, S. Eco-friendly and sustainable synthesis of biocompatible nanomaterials for diagnostic imaging: Current challenges and future perspectives. *Green Chem.* **2020**, *22*, 2662–2687. [[CrossRef](#)]
8. Alavi, M.; Varma, R.S. Phytosynthesis and modification of metal and metal oxide nanoparticles/nanocomposites for antibacterial and anticancer activities: Recent advances. *Sustain. Chem. Pharm.* **2021**, *21*, 100412. [[CrossRef](#)]
9. Shafiee, A.; Iravani, S.; Varma, R.S. Graphene and graphene oxide with anticancer applications: Challenges and future perspectives. *MedComm* **2022**, *3*, e118. [[CrossRef](#)]
10. Delfi, M.; Sartorius, R.; Ashrafizadeh, M.; Sharifi, E.; Zhang, Y.; De Berardinis, P.; Zarrabi, A.; Varma, R.S.; Tay, F.R.; Smith, B.R.; et al. Self-assembled peptide and protein nanostructures for anti-cancer therapy: Targeted delivery, stimuli-responsive devices and immunotherapy. *Nano Today* **2021**, *38*, 101119. [[CrossRef](#)]
11. Rabiee, N.; Bagherzadeh, M.; Ghadiri, A.M.; Fatahi, Y.; Aldhafer, A.; Makvandi, P.; Dinarvand, R.; Jouyandeh, M.; Saeb, M.R.; Mozafari, M.; et al. Turning Toxic Nanomaterials into a Safe and Bioactive Nanocarrier for Co-delivery of DOX/pCRISPR. *ACS Appl. Bio Mater.* **2021**, *4*, 5336–5351. [[CrossRef](#)]
12. Rabiee, N.; Bagherzadeh, M.; Jouyandeh, M.; Zarrintaj, P.; Saeb, M.R.; Mozafari, M.; Shokouhimehr, M.; Varma, R.S. Natural Polymers Decorated MOF-MXene Nanocarriers for Co-delivery of Doxorubicin/pCRISPR. *ACS Appl. Bio Mater.* **2021**, *4*, 5106–5121. [[CrossRef](#)] [[PubMed](#)]
13. Yan, J.; Yao, Y.; Yan, S.; Gao, R.; Lu, W.; He, W. Chiral Protein Supraparticles for Tumor Suppression and Synergistic Immunotherapy: An Enabling Strategy for Bioactive Supramolecular Chirality Construction. *Nano Lett.* **2020**, *20*, 5844–5852. [[CrossRef](#)] [[PubMed](#)]
14. Kim, H.; Beack, S.; Han, S.; Shin, M.; Lee, T.; Park, Y.; Kim, K.S.; Yetisen, A.K.; Yun, S.H.; Kwon, W.; et al. Multifunctional Photonic Nanomaterials for Diagnostic, Therapeutic, and Theranostic Applications. *Adv. Mater.* **2018**, *30*, 1701460. [[CrossRef](#)] [[PubMed](#)]
15. Song, S.; Shen, H.; Wang, Y.; Chu, X.; Xie, J.; Zhou, N.; Shen, J. Biomedical application of graphene: From drug delivery, tumor therapy, to theranostics. *Colloids Surf. B* **2020**, *185*, 110596. [[CrossRef](#)]
16. Qian, X.; Gu, Z.; Chen, Y. Two-dimensional black phosphorus nanosheets for theranostic nanomedicine. *Mater. Horiz.* **2017**, *4*, 800–816. [[CrossRef](#)]
17. Angizi, S.; Alem, S.A.A.; Azar, M.H.; Shayeganfar, F.; Manning, M.I.; Hatamie, A.; Pakdel, A.; Simchi, A. A comprehensive review on planar boron nitride nanomaterials: From 2D nanosheets towards 0D quantum dots. *Prog. Mater. Sci.* **2022**, *124*, 100884. [[CrossRef](#)]
18. Chen, Y.; Wang, L.; Shi, J. Two-dimensional non-carbonaceous materials-enabled efficient photothermal cancer therapy. *Nano Today* **2016**, *11*, 292–308. [[CrossRef](#)]
19. Gong, L.; Yan, L.; Zhou, R.; Xie, J.; Wu, W.; Gu, Z. Two-dimensional transition metal dichalcogenide nanomaterials for combination cancer therapy. *J. Mater. Chem. B* **2017**, *5*, 1873–1895. [[CrossRef](#)]

20. Novoselov, K.S.; Geim, A.K.; Morozov, S.V.; Jiang, D.; Zhang, Y.; Dubonos, S.V.; Grigorieva, I.V.; Firsov, A.A. Electric field effect in atomically thin carbon films. *Science* **2004**, *306*, 666–669. [[CrossRef](#)]
21. Qian, X.; Shen, S.; Liu, T.; Cheng, L.; Liu, Z. Two-dimensional TiS₂ nanosheets for in vivo photoacoustic imaging and photothermal cancer therapy. *Nanoscale* **2015**, *7*, 6380–6387. [[CrossRef](#)]
22. Wang, J.; Sui, L.; Huang, J.; Miao, L.; Nie, Y.; Wang, K.; Yang, Z.; Huang, Q.; Gong, X.; Nan, Y.; et al. MoS₂-based nanocomposites for cancer diagnosis and therapy. *Bioact. Mater.* **2021**, *6*, 4209–4242. [[CrossRef](#)] [[PubMed](#)]
23. Manisekaran, R.; García-Contreras, R.; Rasu Chettiar, A.-D.; Serrano-Díaz, P.; Lopez-Ayuso, C.A.; Arenas-Arocena, M.C.; Hernández-Padrón, G.; López-Marín, L.M.; Acosta-Torres, L.S. 2D Nanosheets—A New Class of Therapeutic Formulations against Cancer. *Pharmaceutics* **2021**, *13*, 1803. [[CrossRef](#)] [[PubMed](#)]
24. Liu, H.; Mei, Y.; Zhao, Q.; Zhang, A.; Tang, L.; Gao, H.; Wang, W. Black Phosphorus, an Emerging Versatile Nanoplatforform for Cancer Immunotherapy. *Pharmaceutics* **2021**, *13*, 1344. [[CrossRef](#)] [[PubMed](#)]
25. Wen, J.; Yang, K.; Huang, J.; Sun, S. Recent advances in LDH-based nanosystems for cancer therapy. *Mater. Des.* **2021**, *198*, 109298. [[CrossRef](#)]
26. Liu, C.; Qin, H.; Kang, L.; Chen, Z.; Wang, H.; Qiu, H.; Ren, J.; Qu, X. Graphitic carbon nitride nanosheets as a multifunctional nanoplatforform for photochemical internalization-enhanced photodynamic therapy. *J. Mater. Chem. B* **2018**, *6*, 7908–7915. [[CrossRef](#)] [[PubMed](#)]
27. Ciofani, M.E.; Şen, Ö.; Çulha, M. Hexagonal Boron Nitride Nanoparticles for Prostate Cancer Treatment. *ACS Appl. Nano Mater.* **2020**, *3*, 2364–2372. [[CrossRef](#)]
28. Saeb, M.R.; Rabiee, N.; Mozafari, M.; Verpoort, F.; Voskressensky, L.G.; Luque, R. Metal–Organic Frameworks (MOFs) for Cancer Therapy. *Materials* **2021**, *14*, 7277. [[CrossRef](#)]
29. Pandey, N.; Dhiman, S.; Srivastava, T.; Majumder, S. Transition metal oxide nanoparticles are effective in inhibiting lung cancer cell survival in the hypoxic tumor microenvironment. *Chem. Biol. Interact.* **2016**, *254*, 221–230. [[CrossRef](#)]
30. Pogorielov, M.; Smyrnova, K.; Kyrylenko, S.; Gogotsi, O.; Zahorodna, V.; Pogrebnjak, A. MXenes—A New Class of Two-Dimensional Materials: Structure, Properties and Potential Applications. *Nanomaterials* **2021**, *11*, 3412. [[CrossRef](#)]
31. Dai, C.; Chen, Y.; Jing, X.; Xiang, L.; Yang, D.; Lin, H.; Liu, Z.; Han, X.; Wu, R. Two-Dimensional Tantalum Carbide (MXenes) Composite Nanosheets for Multiple Imaging-Guided Photothermal Tumor Ablation. *ACS Nano* **2017**, *11*, 12696–12712. [[CrossRef](#)]
32. Han, X.; Huang, J.; Lin, H.; Wang, Z.; Li, P.; Chen, Y. 2D Ultrathin MXene-Based Drug-Delivery Nanoplatforform for Synergistic Photothermal Ablation and Chemotherapy of Cancer. *Adv. Healthc. Mater.* **2018**, *7*, e1701394. [[CrossRef](#)] [[PubMed](#)]
33. Korupalli, C.; You, K.-L.; Getachew, G.; Rasal, A.S.; Dirersa, W.B.; Zakki Fahmi, M.; Chang, J.-Y. Engineering the Surface of Ti₃C₂ MXene Nanosheets for High Stability and Multimodal Anticancer Therapy. *Pharmaceutics* **2022**, *14*, 304. [[CrossRef](#)] [[PubMed](#)]
34. Karthikeyan, P.; Elanchezhyan, S.S.; Preethi, J.; Talukdar, K.; Meenakshi, S.; Park, C.M. Two-dimensional (2D) Ti₃C₂T_x MXene nanosheets with superior adsorption behavior for phosphate and nitrate ions from the aqueous environment. *Ceram. Int.* **2020**, *47*, 732–739. [[CrossRef](#)]
35. Iravani, S.; Varma, R.S. MXenes in cancer nanotheranostics. *Nanomaterials* **2022**, *12*, 3360. [[CrossRef](#)]
36. Zhang, Y.-Z.; El-Demellawi, J.K.; Jiang, Q.; Ge, G.; Liang, H.; Lee, K.; Dong, X.; Alshareef, H.N. MXene hydrogels: Fundamentals and applications. *Chem. Soc. Rev.* **2020**, *49*, 7229–7251. [[CrossRef](#)]
37. Naguib, M.; Kurtoglu, M.; Presser, V.; Lu, J.; Niu, J.; Heon, M.; Hultman, L.; Gogotsi, Y.; Barsoum, M.W. Two-Dimensional Nanocrystals Produced by Exfoliation of Ti₃AlC₂. *Adv. Mater.* **2011**, *23*, 4248–4253. [[CrossRef](#)]
38. Jamalipour Soufi, G.; Iravani, P.; Hekmatnia, A.; Mostafavi, E.; Khatami, M.; Iravani, S. MXenes and MXene-based Materials with Cancer Diagnostic Applications: Challenges and Opportunities. *Comments Inorg. Chem.* **2021**, *42*, 174–207. [[CrossRef](#)]
39. Nguyen, T.P.; Nguyen, D.M.T.; Le, H.K.; Vo, D.-V.N.; Lam, S.S.; Varma, R.S.; Shokouhimehr, M.; Nguyen, C.C.; Van Le, Q. MXenes: Applications in electrocatalytic, photocatalytic hydrogen evolution reaction and CO₂ reduction. *Mol. Catal.* **2020**, *486*, 110850. [[CrossRef](#)]
40. Malaki, M.; Maleki, A.; Varma, R.S. MXenes and ultrasonication. *J. Mater. Chem. A* **2019**, *7*, 10843–10857. [[CrossRef](#)]
41. Eid, K.; Lu, Q.; Abdel-Azeim, S.; Soliman, A.; Abdullah, A.M.; Abdelgwad, A.M.; Forbes, R.P.; Ozoemena, K.I.; Varma, R.S.; Shibl, M.F. Highly exfoliated Ti₃C₂T_x MXene nanosheets atomically doped with Cu for efficient electrochemical CO₂ reduction: An experimental and theoretical study. *J. Mater. Chem. A* **2022**. [[CrossRef](#)]
42. Ma, L.; Ting, L.R.L.; Molinari, V.; Giordano, C.; Yeo, B.S. Efficient hydrogen evolution reaction catalyzed by molybdenum carbide and molybdenum nitride nanocatalysts synthesized via the urea glass route. *J. Mater. Chem. A* **2015**, *3*, 8361–8368. [[CrossRef](#)]
43. Xu, C.; Wang, L.; Liu, Z.; Chen, L.; Guo, J.; Kang, N.; Ma, X.-L.; Cheng, H.-M.; Ren, W. Large-area high-quality 2D ultrathin Mo₂C superconducting crystals. *Nat. Mater.* **2015**, *14*, 1135–1141. [[CrossRef](#)] [[PubMed](#)]
44. Urbankowski, P.; Anasori, B.; Makaryan, T.; Er, D.; Kota, S.; Walsh, P.L.; Zhao, M.; Shenoy, V.B.; Barsoum, M.W.; Gogotsi, Y. Synthesis of two-dimensional titanium nitride Ti₄N₃ (MXene). *Nanoscale* **2016**, *8*, 11385–11391. [[CrossRef](#)] [[PubMed](#)]
45. Li, T.; Yao, L.; Liu, Q.; Gu, J.; Luo, R.; Li, J.; Yan, X.; Wang, W.; Liu, P.; Chen, B. Fluorine-free synthesis of high-purity Ti₃C₂T_x (T = OH, O) via alkali treatment. *Angew. Chem. Int. Ed.* **2018**, *57*, 6115–6119. [[CrossRef](#)]
46. Sun, W.; Shah, S.; Chen, Y.; Tan, Z.; Gao, H.; Habib, T.; Radovic, M.; Green, M. Electrochemical etching of Ti₂AlC to Ti₂CT_x (MXene) in low-concentration hydrochloric acid solution. *J. Mater. Chem. A* **2017**, *5*, 21663–21668. [[CrossRef](#)]
47. Iravani, S.; Varma, R.S. MXenes in photomedicine: Advances and prospects. *ChemComm* **2022**, *58*, 7336–7350. [[CrossRef](#)]

48. Iravani, S.; Varma, R.S. MXenes for Cancer Therapy and Diagnosis: Recent Advances and Current Challenges. *ACS Biomater. Sci. Eng.* **2021**, *7*, 1900–1913. [[CrossRef](#)]
49. Kuang, P.; Low, J.; Cheng, B.; Yu, J.; Fan, J. MXene-based photocatalysts. *J. Mater. Sci. Technol.* **2020**, *56*, 18–44. [[CrossRef](#)]
50. Wang, C.; Wang, Y.; Jiang, X.; Xu, J.; Huang, W.; Zhang, F.; Liu, J.; Yang, F.; Song, Y.; Ge, Y.; et al. MXene $Ti_3C_2T_x$: A Promising Photothermal Conversion Material and Application in All-Optical Modulation and All-Optical Information Loading. *Adv. Opt. Mater.* **2019**, *7*, 1900060. [[CrossRef](#)]
51. Hendijani, F. Human mesenchymal stromal cell therapy for prevention and recovery of chemo/radiotherapy adverse reactions. *Cytotherapy* **2015**, *17*, 509–525. [[CrossRef](#)]
52. Pardoll, D.M. The blockade of immune checkpoints in cancer immunotherapy. *Nat. Rev. Cancer* **2012**, *12*, 252–264. [[CrossRef](#)] [[PubMed](#)]
53. Chari, R.V.J. Targeted Cancer Therapy: Conferring Specificity to Cytotoxic Drugs. *Acc. Chem. Res.* **2007**, *41*, 98–107. [[CrossRef](#)] [[PubMed](#)]
54. Murugan, C.; Sharma, V.; Murugan, R.K.; Malaimengu, G.; Sundaramurthy, A. Two-dimensional cancer theranostic nanomaterials: Synthesis, surface functionalization and applications in photothermal therapy. *J. Control. Release* **2019**, *299*, 1–20. [[CrossRef](#)] [[PubMed](#)]
55. Shi, Z.; Zhou, Y.; Fan, T.; Lin, Y.; Zhang, H.; Mei, L. Inorganic nano-carriers based smart drug delivery systems for tumor therapy. *Smart Mater. Med.* **2020**, *1*, 32–47. [[CrossRef](#)]
56. Jain, V.; Jain, S.; Mahajan, S. Nanomedicines Based Drug Delivery Systems for Anti-Cancer Targeting and Treatment. *Curr. Drug Deliv.* **2015**, *12*, 177–191. [[CrossRef](#)]
57. Iravani, P.; Iravani, S.; Varma, R.S. MXene-chitosan composites and their biomedical potentials. *Micromachines* **2022**, *13*, 1383. [[CrossRef](#)]
58. Lin, H.; Chen, Y.; Shi, J. Insights into 2D MXenes for Versatile Biomedical Applications: Current Advances and Challenges Ahead. *Adv. Sci.* **2018**, *5*, 1800518. [[CrossRef](#)]
59. George, S.M.; Kandasubramanian, B. Advancements in MXene-Polymer composites for various biomedical applications. *Ceram. Int.* **2019**, *46*, 8522–8535. [[CrossRef](#)]
60. Alhussain, H.; Augustine, R.; Hussein, E.A.; Gupta, I.; Hasan, A.; Al Moustafa, A.-E.; Elzatahry, A. MXene Nanosheets May Induce Toxic Effect on the Early Stage of Embryogenesis. *J. Biomed. Nanotechnol.* **2020**, *16*, 364–372. [[CrossRef](#)]
61. Iravani, S.; Varma, R.S. Bioinspired and biomimetic MXene-based structures with fascinating properties: Recent advances. *Mater. Adv.* **2022**, *3*, 4783–4796. [[CrossRef](#)]
62. Huang, H.; Dong, C.; Feng, W.; Wang, Y.; Huang, B.; Chen, Y. Biomedical engineering of two-dimensional MXenes. *Adv. Drug Deliv. Rev.* **2022**, *184*, 114178. [[CrossRef](#)] [[PubMed](#)]
63. Zamhuri, A.; Lim, G.P.; Ma, N.L.; Tee, K.S.; Soon, C.F. MXene in the lens of biomedical engineering: Synthesis, applications and future outlook. *Biomed. Eng. Online* **2021**, *20*, 33. [[CrossRef](#)] [[PubMed](#)]
64. Shukla, V. Review of electromagnetic interference shielding materials fabricated by iron ingredients. *Nanoscale Adv.* **2019**, *1*, 1640–1671. [[CrossRef](#)] [[PubMed](#)]
65. Zhan, X.; Si, C.; Zhou, J.; Sun, Z. MXene and MXene-based composites: Synthesis, properties and environment-related applications. *Nanoscale Horiz.* **2019**, *5*, 235–258. [[CrossRef](#)]
66. Verger, L.; Xu, C.; Natu, V.; Cheng, H.-M.; Ren, W.; Barsoum, M.W. Overview of the synthesis of MXenes and other ultrathin 2D transition metal carbides and nitrides. *Curr. Opin. Solid State Mater. Sci.* **2019**, *23*, 149–163. [[CrossRef](#)]
67. Rozmysłowska-Wojciechowska, A.; Mitrzak, J.; Szuplewska, A.; Chudy, M.; Woźniak, J.; Petrus, M.; Wojciechowski, T.; Vasilchenko, A.S.; Jastrzębska, A.M. Engineering of 2D Ti_3C_2 MXene Surface Charge and its Influence on Biological Properties. *Materials* **2020**, *13*, 2347. [[CrossRef](#)]
68. Xing, C.; Chen, S.; Liang, X.; Liu, Q.; Qu, M.; Zou, Q.; Li, J.; Tan, H.; Liu, L.; Fan, D.; et al. Two-Dimensional MXene (Ti_3C_2)-Integrated Cellulose Hydrogels: Toward Smart Three-Dimensional Network Nanoplatfoms Exhibiting Light-Induced Swelling and Bimodal Photothermal/Chemotherapy Anticancer Activity. *ACS Appl. Mater. Interfaces* **2018**, *10*, 27631–27643. [[CrossRef](#)]
69. Xie, Y.; Naguib, M.; Mochalin, V.N.; Barsoum, M.W.; Gogotsi, Y.; Yu, X.; Nam, K.-W.; Yang, X.-Q.; Kolesnikov, A.I.; Kent, P.R. Role of Surface Structure on Li-Ion Energy Storage Capacity of Two-Dimensional Transition-Metal Carbides. *J. Am. Chem. Soc.* **2014**, *136*, 6385–6394. [[CrossRef](#)]
70. Xie, Y.; Dall’Agnese, Y.; Naguib, M.; Gogotsi, Y.; Barsoum, M.W.; Zhuang, H.L.; Kent, P.R.C. Prediction and Characterization of MXene Nanosheet Anodes for Non-Lithium-Ion Batteries. *ACS Nano* **2014**, *8*, 9606–9615. [[CrossRef](#)]
71. Hu, T.; Wang, J.; Zhang, H.; Li, Z.; Hu, M.; Wang, X. Vibrational properties of Ti_3C_2 and $Ti_3C_2T_2$ (T = O, F, OH) monosheets by first-principles calculations: A comparative study. *Phys. Chem. Chem. Phys.* **2015**, *17*, 9997–10003. [[CrossRef](#)]
72. Tang, Q.; Zhou, Z.; Shen, P. Are MXenes Promising Anode Materials for Li Ion Batteries? Computational Studies on Electronic Properties and Li Storage Capability of Ti_3C_2 and $Ti_3C_2X_2$ (X = F, OH) Monolayer. *J. Am. Chem. Soc.* **2012**, *134*, 16909–16916.
73. Khazaei, M.; Arai, M.; Sasaki, T.; Chung, C.-Y.; Venkataramanan, N.S.; Estili, M.; Sakka, Y.; Kawazoe, Y. Novel Electronic and Magnetic Properties of Two-Dimensional Transition Metal Carbides and Nitrides. *Adv. Funct. Mater.* **2012**, *23*, 2185–2192. [[CrossRef](#)]
74. Wang, X.; Shen, X.; Gao, Y.; Wang, Z.; Yu, R.; Chen, L. Atomic-Scale Recognition of Surface Structure and Intercalation Mechanism of Ti_3C_2X . *J. Am. Chem. Soc.* **2015**, *137*, 2715–2721. [[CrossRef](#)] [[PubMed](#)]

75. Enyashin, A.N.; Ivanovskii, A.L. Two-dimensional titanium carbonitrides and their hydroxylated derivatives: Structural, electronic properties and stability of MXenes $Ti_3C_2-xN_x(OH)_2$ from DFTB calculations. *J. Solid State Chem.* **2013**, *207*, 42–48. [[CrossRef](#)]
76. Mauchamp, V.; Bugnet, M.; Bellido, E.P.; Botton, G.A.; Moreau, P.; Magne, D.; Naguib, M.; Cabioch, T.; Barsoum, M.W. Enhanced and tunable surface plasmons in two-dimensional Ti_3C_2 stacks: Electronic structure versus boundary effects. *Phys. Rev. B* **2014**, *89*, 235428. [[CrossRef](#)]
77. Shein, I.R.; Ivanovskii, A.L. Planar nano-block structures $Ti_{n+1}Al_{0.5}C_n$ and $Ti_{n+1}C_n$ ($n = 1, \text{ and } 2$) from MAX phases: Structural, electronic properties and relative stability from first principles calculations. *Superlattices Microstruct.* **2012**, *52*, 147–157. [[CrossRef](#)]
78. Shein, I.R.; Ivanovskii, A.L. Graphene-like titanium carbides and nitrides $Ti_{n+1}C_n$, $Ti_{n+1}N_n$ ($n = 1, 2, \text{ and } 3$) from de-intercalated MAX phases: First-principles probing of their structural, electronic properties and relative stability. *Comput. Mater. Sci.* **2012**, *65*, 104–114. [[CrossRef](#)]
79. Xie, Y.; Kent, P.R.C. Hybrid density functional study of structural and electronic properties of functionalized $Ti_{n+1}X_n$ ($X = C, N$) monolayers. *Phys. Rev. B* **2013**, *87*, 235441. [[CrossRef](#)]
80. Zhao, S.; Kang, W.; Xue, J. Manipulation of electronic and magnetic properties of M_2C ($M = Hf, Nb, Sc, Ta, Ti, V, Zr$) monolayer by applying mechanical strains. *Appl. Phys. Lett.* **2014**, *104*, 133106. [[CrossRef](#)]
81. Wang, S.; Li, J.-X.; Du, Y.-L.; Cui, C. First-principles study on structural, electronic and elastic properties of graphene-like hexagonal Ti_2C monolayer. *Comput. Mater. Sci.* **2014**, *83*, 290–293. [[CrossRef](#)]
82. Khazaei, M.; Arai, M.; Sasaki, T.; Estili, M.; Sakka, Y. Two-dimensional molybdenum carbides: Potential thermoelectric materials of the MXene family. *Phys. Chem. Chem. Phys.* **2014**, *16*, 7841–7849. [[CrossRef](#)] [[PubMed](#)]
83. Lashgari, H.; Abolhassani, M.R.; Boochani, A.; Elahi, S.M.; Khodadadi, J. Electronic and optical properties of 2D graphene-like compounds titanium carbides and nitrides: DFT calculations. *Solid State Commun.* **2014**, *195*, 61–69. [[CrossRef](#)]
84. Enyashin, A.N.; Ivanovskii, A.L. Structural and Electronic Properties and Stability of MXenes Ti_2C and Ti_3C_2 Functionalized by Methoxy Groups. *J. Phys. Chem. C* **2013**, *117*, 13637–13643. [[CrossRef](#)]
85. Naguib, M.; Mashtalir, O.; Lukatskaya, M.R.; Dyatkin, B.; Zhang, C.; Presser, V.; Gogotsi, Y.; Barsoum, M.W. One-step synthesis of nanocrystalline transition metal oxides on thin sheets of disordered graphitic carbon by oxidation of MXenes. *Chem. Commun.* **2014**, *50*, 7420–7423. [[CrossRef](#)]
86. Johnson, K.K.; Koshy, P.; Yang, J.L.; Sorrell, C.C. Preclinical Cancer Theranostics—From Nanomaterials to Clinic: The Missing Link. *Adv. Funct. Mater.* **2021**, *31*, 2104199. [[CrossRef](#)]
87. Ghidui, M.; Lukatskaya, M.R.; Zhao, M.-Q.; Gogotsi, Y.; Barsoum, M.W. Conductive two-dimensional titanium carbide ‘clay’ with high volumetric capacitance. *Nature* **2014**, *516*, 78–81. [[CrossRef](#)]
88. Shahzad, F.; Alhabeib, M.; Hatter, C.B.; Anasori, B.; Man Hong, S.; Koo, C.M.; Gogotsi, Y. Electromagnetic interference shielding with 2D transition metal carbides (MXenes). *Science* **2016**, *353*, 1137–1140. [[CrossRef](#)]
89. Montazeri, K.; Currie, M.; Verger, L.; Dianat, P.; Barsoum, M.W.; Nabet, B. Beyond Gold: Spin-Coated Ti_3C_2 -Based MXene Photodetectors. *Adv. Mater.* **2019**, *31*, 1903271. [[CrossRef](#)]
90. Naguib, M.; Mochalin, V.N.; Barsoum, M.W.; Gogotsi, Y. Two-dimensional materials: 25th anniversary article: MXenes: A new family of two-dimensional materials (Adv. Mater. 7/2014). *Adv. Mater.* **2014**, *26*, 982. [[CrossRef](#)]
91. Dillon, A.D.; Ghidui, M.J.; Krick, A.L.; Griggs, J.; May, S.J.; Gogotsi, Y.; Barsoum, M.W.; Fafarman, A.T. Highly Conductive Optical Quality Solution-Processed Films of 2D Titanium Carbide. *Adv. Funct. Mater.* **2016**, *26*, 4162–4168. [[CrossRef](#)]
92. Dai, C.; Lin, H.; Xu, G.; Liu, Z.; Wu, R.; Chen, Y. Biocompatible 2D titanium carbide (MXenes) composite nanosheets for pH-responsive MRI-guided tumor hyperthermia. *Chem. Mater.* **2017**, *29*, 8637–8652. [[CrossRef](#)]
93. Loo, T.W.; Clarke, D. Recent Progress in Understanding the Mechanism of P-Glycoprotein-mediated Drug Efflux. *J. Membr. Biol.* **2005**, *206*, 173–185. [[CrossRef](#)] [[PubMed](#)]
94. Hao, Z.; Li, Y.; Liu, X.; Jiang, T.; He, Y.; Zhang, X.; Cong, C.; Wang, D.; Liu, Z.; Gao, D. Enhancing biocatalysis of a MXene-based biomimetic plasmonic assembly for targeted cancer treatments in NIR-II biowindow. *Chem. Eng. J.* **2021**, *425*, 130639. [[CrossRef](#)]
95. Xu, Y.; Wang, Y.; An, J.; Sedgwick, A.C.; Li, M.; Xie, J.; Hu, W.; Kang, J.; Sen, S.; Steinbrueck, A.; et al. 2D-ultrathin MXene/DOXjade platform for iron chelation chemo-photothermal therapy. *Bioact. Mater.* **2021**, *14*, 76–85. [[CrossRef](#)] [[PubMed](#)]
96. Lin, H.; Wang, X.; Yu, L.; Chen, Y.; Shi, J. Two-Dimensional Ultrathin MXene Ceramic Nanosheets for Photothermal Conversion. *Nano Lett.* **2017**, *17*, 384–391. [[CrossRef](#)]
97. Li, M.; Shao, Y.; Kim, J.H.; Pu, Z.; Zhao, X.; Huang, H.; Xiong, T.; Kang, Y.; Li, G.; Shao, K.; et al. Unimolecular Photodynamic O_2 -Economizer To Overcome Hypoxia Resistance in Phototherapeutics. *J. Am. Chem. Soc.* **2020**, *142*, 5380–5388. [[CrossRef](#)]
98. Li, M.; Xiong, T.; Du, J.; Tian, R.; Xiao, M.; Guo, L.; Long, S.; Fan, J.; Sun, W.; Shao, K.; et al. Superoxide Radical Photogenerator with Amplification Effect: Surmounting the Achilles’ Heels of Photodynamic Oncotherapy. *J. Am. Chem. Soc.* **2019**, *141*, 2695–2702. [[CrossRef](#)]
99. Gupta, P.; Jat, K.; Solanki, V.S.; Shrivastava, R. Synthesis and Antimicrobial Activity of some New N’-Arylidene-4-(3, 5-Bis (2-Hydroxyphenyl)-1H-1, 2, 4-Triazole-1-yl) Benzohydrazides. *Indian J. Heterocycl. Chem.* **2017**, *27*, 151–156.
100. Zhang, X.; Cheng, L.; Lu, Y.; Tang, J.; Lv, Q.; Chen, X.; Chen, Y.; Liu, J. A MXene-Based Bionic Cascaded-Enzyme Nanoreactor for Tumor Phototherapy/Enzyme Dynamic Therapy and Hypoxia-Activated Chemotherapy. *Nano-Micro Lett.* **2021**, *14*, 22. [[CrossRef](#)]
101. Sun, K.-Y.; Wu, Y.; Xu, J.; Xiong, W.; Xu, W.; Li, J.; Sun, Z.; Lv, Z.; Wu, X.S.; Jiang, Q.; et al. Niobium carbide (MXene) reduces UHMWPE particle-induced osteolysis. *Bioact. Mater.* **2022**, *8*, 435–448. [[CrossRef](#)]

102. Feng, X.; Li, M.; Wang, J.; Zou, X.; Wang, H.; Wang, D.; Zhou, H.; Yang, L.; Gao, W.; Liang, C. MXene Quantum Dot/Zeolitic Imidazolate Framework Nanocarriers for Dual Stimulus Triggered Tumor Chemo-Phototherapy. *Materials* **2022**, *15*, 4543. [[CrossRef](#)] [[PubMed](#)]
103. Liu, J.; Qiao, S.Z.; Chen, J.S.; Lou, X.W.D.; Xing, X.; Lu, G.Q.M. Yolk/shell nanoparticles: New platforms for nanoreactors, drug delivery and lithium-ion batteries. *Chem. Commun.* **2011**, *47*, 12578–12591. [[CrossRef](#)] [[PubMed](#)]
104. Lu, B.; Hu, S.; Wu, D.; Wu, C.; Zhu, Z.; Hu, L.; Zhang, J. Ionic liquid exfoliated $Ti_3C_2T_x$ MXene nanosheets for photoacoustic imaging and synergistic photothermal/chemotherapy of cancer. *J. Mater. Chem. B* **2022**, *10*, 1226–1235. [[CrossRef](#)] [[PubMed](#)]
105. Hanušová, V.; Boušová, I.; Skálová, L. Possibilities to increase the effectiveness of doxorubicin in cancer cells killing. *Drug Metab. Rev.* **2011**, *43*, 540–557. [[CrossRef](#)]
106. Liu, A.; Liu, Y.; Liu, G.; Zhang, A.; Cheng, Y.; Li, Y.; Zhang, L.; Wang, L.; Zhou, H.; Liu, J.; et al. Engineering of surface modified $Ti_3C_2T_x$ MXene based dually controlled drug release system for synergistic multitherapies of cancer. *Biochem. Eng. J.* **2022**, *448*, 137691. [[CrossRef](#)]